

displayed again in Fig. 4, along with similar projections of the data at two other angles. In this figure the locus of  $E_{12}^- = 600$  keV has been drawn in on the  $T_f$ ,  $T_m$  plane, showing a peaking of intensity in this region corresponding to a proton-proton interaction of some 600 keV. The unexpected energy and widths of the peaks perhaps indicates an interference effect, similar

to that discussed by Phillips<sup>5</sup> and Bronson,<sup>3</sup> causing the separation and narrowing of these peaks which probably correspond to a broader, lower internal energy interaction than that observed.

<sup>5</sup> G. C. Phillips, Rev. Mod. Phys. **36**, 1085 (1964); G. C. Phillips, paper in this conference, Rev. Mod. Phys. **37**, 409 (1965).

## $D(p, 2p)n$ Reaction at 31 MeV\*

S. M. BUNCH, C. C. KIM, H. H. FORSTER

*University of Southern California, Los Angeles, California*

### I. INTRODUCTION

Studies involving the interaction of protons with deuterons are important because of the interest in nucleon-nucleon interactions, three-body forces, and deuteron states. In addition, the fact that the deuteron is so loosely bound permits one to use certain approximations which cannot ordinarily be made in the theoretical treatment of nuclear reactions.

The nucleon-deuteron breakup problem has been formulated in the Born approximation by several investigators,<sup>1-4</sup> and in the impulse approximation by Chew.<sup>5</sup> The direct application of either of these approaches is quite difficult; but the approximations suggested by Frank and Gammel,<sup>6</sup> and Kuckes, Wilson, and Cooper<sup>7</sup> can be more easily applied. The first of these relates the  $D(p, 2p)n$  reaction to  $p$ - $d$  scattering, while in the second, the neutron is treated as a spectator particle.

Experimentally, the breakup of the deuteron following proton bombardment has been investigated over a wide range of incident proton energies.<sup>6,8-13</sup> However, scattering experiments involving the detection of one outgoing particle do not seem to lead to conclusive information.

\* Work supported in part by the U.S. Atomic Energy Commission.

<sup>1</sup> T. Y. Wu and J. Ashkin, Phys. Rev. **73**, 986 (1948).

<sup>2</sup> G. F. Chew, Phys. Rev. **74**, 809 (1948).

<sup>3</sup> F. de Hoffman, Phys. Rev. **78**, 216 (1950).

<sup>4</sup> R. L. Gluckstern and H. A. Bethe, Phys. Rev. **81**, 761 (1951).

<sup>5</sup> G. F. Chew, Phys. Rev. **80**, 196 (1950).

<sup>6</sup> R. M. Frank and J. L. Gammel, Phys. Rev. **93**, 463 (1954).

<sup>7</sup> A. F. Kuckes, R. Wilson, and P. F. Cooper, Jr., Ann. Phys. (N. Y.) **15**, 193 (1961).

<sup>8</sup> W. H. Barkas and M. G. White, Phys. Rev. **56**, 288 (1939).

<sup>9</sup> L. Cranberg and R. K. Smith, Phys. Rev. **113**, 587 (1959).

<sup>10</sup> S. Kikuchi, J. Sanada, S. Suwa, I. Hayashi, K. Nisimura, and K. Fukunaga, J. Phys. Soc. Japan **15**, 749 (1960).

<sup>11</sup> K. Nisimura, J. Phys. Soc. Japan **16**, 2097 (1961).

<sup>12</sup> W. T. H. Van Oers and K. W. Brockman, Nucl. Phys. **47**, 338 (1963).

<sup>13</sup> D. G. Stairs, R. Wilson, and P. F. Cooper, Jr., Phys. Rev. **129**, 1672 (1963).

Recently angular correlations of coincident protons emitted in the deuteron breakup have been studied at 18 MeV,<sup>14</sup> 50 MeV,<sup>15</sup> and 145 MeV.<sup>16</sup> Of these, only the 145-MeV data agreed with the predictions of the spectator model; for the lower energy experiments the difference between the simple predictions of the model and the experimental data was considerable; nor was an analysis of the 18-MeV results with a Frank-Gammel calculation more successful.

### II. EXPERIMENTAL PROCEDURE

The 31-MeV proton beam of the University of Southern California linear accelerator was used to bombard a gaseous deuterium target. The scattering chamber has previously been described in detail,<sup>16</sup> except that it was modified by the insertion of a rotating, O-ring vacuum seal in the top through which the size of an internal collimator was controlled. Solid targets for calibration purposes could be inserted into the beam line from the bottom of the chamber.

The collimated proton beam, after leaving the end of the beam pipe which consisted of a  $\frac{1}{4}$ -in.-diam nickel collimator and a 0.002-in. Al window, passed through  $\frac{1}{2}$  in. of air and a 0.001-in. Al chamber window into the chamber filled with 99.5% pure deuterium gas, at a pressure of 200–600 Torr. Charge collection took place in a Faraday cup placed behind the chamber. The scattered particles were stopped and detected by 1-in. NaI(Tl) crystals mounted onto 6655A photomultiplier tubes. One scattering arm was fixed at 35° and the other was continuously variable. In the fixed scattering arm (upper arm), the particle passed through a 60- $\mu$  surface-barrier solid-state detector. The geometry was determined by  $\frac{3}{4}$ -in.-diam collimators placed directly in front of the NaI(Tl) crystals. These collimators were

<sup>14</sup> R. E. Warner, Phys. Rev. **132**, 2621 (1963).

<sup>15</sup> R. J. Griffiths and K. M. Knight, Nucl. Phys. **54**, 56 (1964).

<sup>16</sup> C. C. Kim, S. M. Bunch, D. W. Devins, and H. H. Forster, Nucl. Phys. (to be published).

located about 7 in. from the center of the scattering chamber. Slit collimators of  $\frac{3}{8}$ -in. width in the fixed arm, and  $\frac{1}{4}$ -in. to 2-in. variable width in the movable arm were located about 4 in. from the center of the chamber and were used for the purpose of defining the sensitive gas volume.

The signals from both the NaI(Tl) detectors and the transmission counter were amplified using conventional electronic circuits. In addition to the slow output, a fast output from both NaI(Tl) detectors was amplified with wide band amplifiers, standardized with tunnel diode discriminators, and put into a tunnel diode fast coincidence circuit, having a time resolution of 15 nsec. The output of the latter was used, in conjunction with the system logic, to gate one or two differential pulse-height analyzers. Electronic block diagrams of two of the systems used are shown in Figs. 1 and 2. In these figures the symbols HP and VGVD refer,

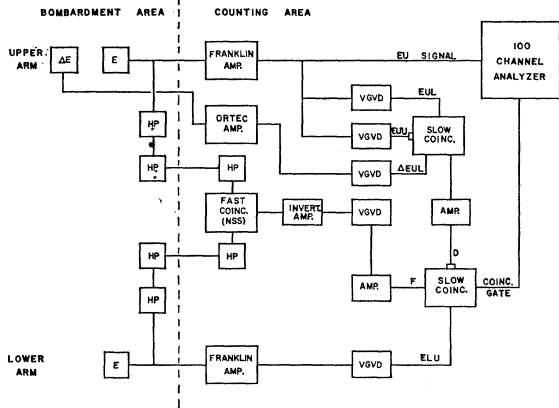


FIG. 1. Block diagram of electronics using coincidence-anti-coincidence logic.

respectively, to the wide band amplifiers and the variable gate-variable delay circuits which were used in this experiment. In the arrangement shown in Fig. 1 the separation of the proton and the deuteron counts is accomplished by means of a coincidence-anticoincidence technique, making use of the energy loss relationship for charged particles in the silicon detector. A coincidence gate is obtained for protons which are in fast coincidence. In addition, the signal labeled ELU is used to eliminate accidental coincidences between the elastic proton peak in the lower arm and a count in the continuum in the other arm. Figure 3 shows the energy loss in the silicon detector as a function of particle energy for both the proton and the deuteron. The lines labeled EUL, EUU, and  $\Delta EUL$  indicate how the respective discriminators shown in Fig. 1 were set. An output *D* was obtained only if the EU signal was in the range EUL to EUU, and the  $\Delta E$  signal was above  $\Delta EUL$ . This output was then used to veto counts from the fast coincidence circuit.

Subsequently this arrangement was replaced by that

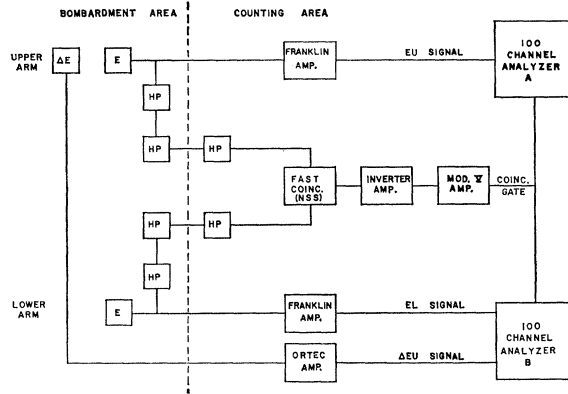


FIG. 2. Block diagram of electronics using two-dimensional analysis.

shown in Fig. 2, in which two 100-channel analyzers were modified so that upon receipt of a coincidence gate from the fast coincidence system, they would immediately print out the channels in which the coincidence occurred. The coincidence counting rates were slow enough so that no substantial losses occurred because of this arrangement and the small loss rate which did occur was easily corrected for. Analyzer A displayed the fixed arm energy (minus the small energy loss in the  $\Delta E$  detector) while analyzer B displayed either  $\Delta E$  or the energy of the particle in the other arm. Both methods gave good separation between protons and deuterons.

The fast coincidence circuitry was adjusted by putting a deuterated polyethylene target into the scattering chamber and setting both detector arms at  $52^\circ$ . In this way the coincidence between the proton elastically scattered from deuterium and its recoil deuteron could be observed. For the two-dimensional calibration, when the  $E-\Delta E$  system was used, both scattering arms were varied in position, but in such a manner that the elastically scattered proton was always in coincidence with its recoil. By this method, a calibration curve was obtained which had the general ap-

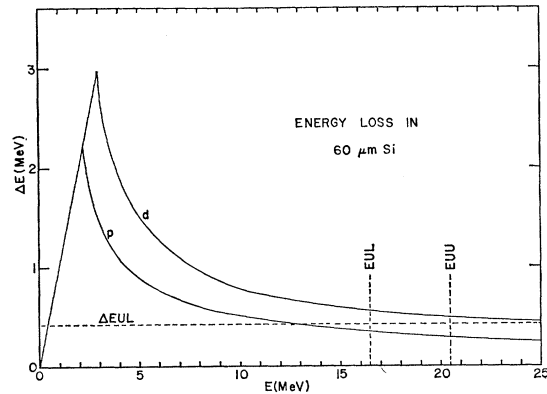


FIG. 3.  $\Delta E-E$  curves using a  $60\text{-}\mu$  silicon absorber. Vertical dashed lines indicate the setting of the discriminators.

pearance of Fig. 3. For the EU-EL system, it was only necessary to make separate energy calibrations for both detectors making use of the kinematical relationship for  $p$ - $d$  scattering.

### III. RESULTS AND DISCUSSION

The calculation of experimental laboratory cross sections for a gas geometry has been discussed elsewhere,<sup>17-19</sup> and only slight modification was necessary in order to apply the same results to a coincidence experiment. In Fig. 4 the differential cross section  $d^2\sigma/d\omega_3 d\omega_4$  is plotted in the laboratory system as a

$$\frac{d^2\sigma}{d\omega_3 d\omega_4 dE_3} = \frac{4\sqrt{2}(E_\alpha E_\beta)^{\frac{1}{2}}[(E_\alpha)^{\frac{1}{2}} + (E_\beta)^{\frac{1}{2}}]^3 (E_\beta)^{\frac{1}{2}} E_4 (d\sigma/d\omega_3)'}{\pi^2 (E_\alpha + 2E_\beta)^2 (E_1)^{\frac{1}{2}} (E_\beta + 2E_5)^2 [2(E_4)^{\frac{1}{2}} - (E_1)^{\frac{1}{2}} \cos \theta_4 + (E_5)^{\frac{1}{2}} \cos(\theta_4 - \theta_3)]^2}, \quad (1)$$

where  $E_\alpha = -2.226$  MeV is the deuteron binding energy,  $E_\beta = 59.8$  MeV;  $E_1$ ,  $E_3$ ,  $E_4$ , and  $E_5$  refer, respectively, to the beam energy, the energy of the proton in the fixed detector, the energy of the proton in the moving detector, and the energy of the recoil neutron, all calculated in the laboratory system;  $\theta_3 = 35^\circ$ ,  $25^\circ \leq \theta_4 \leq 65^\circ$ , and  $(d\sigma/d\omega_3)'$  is the free  $p$ - $p$  elastic scattering cross section in the c.m. system corresponding to a laboratory angle of  $35^\circ$ .

The above expression was integrated over  $E_3$  using a Honeywell 800 computer, and the resulting angular correlation is represented in Fig. 4 together with the experimental data. The three curves represent three

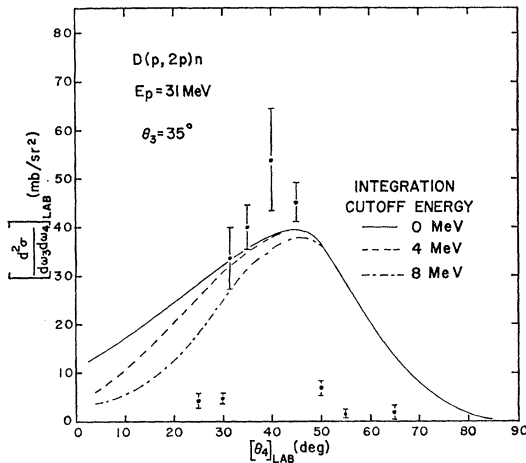


FIG. 4. Angular correlation curves integrated over energy. Points correspond to experimental data, curves to theoretical calculation.

<sup>17</sup> C. L. Critchfield and D. C. Dodder, Phys. Rev. **75**, 419 (1949).

<sup>18</sup> L. H. Johnstone and D. A. Swenson, Phys. Rev. **111**, 212 (1958).

<sup>19</sup> S. M. Bunch, H. H. Forster, and C. C. Kim, Nucl. Phys. **53**, 241 (1964).

function of the angular setting of the movable detector; the fixed detector was at an angle of  $35^\circ$  relative to the incident beam. The dots represent the experimental results, which have been corrected for the effect of finite angular resolution. The errors indicated correspond to absolute standard deviations.

The experimental results were compared with those obtained by applying the spectator model of Kuckes *et al.*<sup>7</sup> to the  $D(p, 2p)n$  reaction at 31 MeV. Using the impulse approximation with plane waves in the final states, and employing the Hulthén wave function for the deuteron, Kuckes obtains the following expression for the differential cross section:

different distributions obtained by varying the low energy integration cutoff point; the solid curve corresponds to a cutoff at 0 MeV, the dashed curve to a cutoff at 4 MeV, and the dot-dash curve to one at 8 MeV.

As can be seen from a comparison of the experimental and calculated distributions none of the three curves fit the experimental data too well; the general shapes of the angular distributions have a certain similarity, in that the position of the maximum is roughly reproduced, but the magnitude of the cross sections at the maximum is less than the experimentally determined value. But the greatest difference between the experimental and theoretical distributions occurs in the rapid decrease in the experimental cross sections when moving away from the maximum as compared to the calculated values. It appears that increasing the cutoff energy from 0-8 MeV somewhat improved the fit in this respect; the experimental cutoff energy was 7 MeV.

A comparison of the experimental results with those obtained at other energies<sup>7,14,15</sup> seems to indicate that with the exception of the high energy data the agreement with the cross sections calculated by the use of the impulse approximation is only fair, indicating possibly that at energies below  $\sim 100$  MeV the approximation is less reliable.

### ACKNOWLEDGMENTS

The authors wish to express their sincere thanks and appreciation to Dr. R. Eisberg and Dr. B. L. Scott for many stimulating discussions, to Dr. D. W. Devins and J. Hoxhikian for assistance in data taking, to Earl I. White and T. K. Inman and the crew of the USC Linear Accelerator for the effective operation of the machine during the experiment, and to the staff of the USC Computer Sciences Laboratory for assistance with the calculations.